Biochimica et Biophysica Acta, 1146 (1993) 87–96

BBAMEM 75887

Quantitative measurement of cationic fluxes, selectivity and membrane potential using liposomes multilabelled with fluorescent probes

Kees Venema, Rémy Gibrat, Jean-Pierre Grouzis and Claude Grignon

Laboratoire de Biochimie et Physiologie Végétales, ENSA / INRA / CNRS (URA 573), Montpellier (France)

(Received 9 September 1992)

Key words: Liposome; Ion flux; Membrane potential; Permeability; Fluorescent probe; PBFI; Oxonol; Pyranine

Liposomes of egg PC/PG (8:2, mol/mol) were multilabelled with PBFI, pyranine and oxonol VI, fluorescent probes for, respectively, K^+, H^+ and membrane potential. Monitoring fluorescence with a multichannel photoncounting spectrofluorometer during K^+ filling experiments allowed to measure K^+ influx, the associated H^+ efflux and the membrane potential, continuously and simultaneously. The proton net efflux quantitatively mirrored the K^+ net influx. The rate of the K^+/H^+ exchange diminished progressively as a quasi-equilibrium was reached for both K^+ and H^+. In the presence of valinomycin, the measured membrane potential during the K^+ filling actually corresponded to the Nernst potential calculated from the observed K^+ gradient. In the absence of valinomycin, it corresponded to the Nernst potential calculated from the observed H^+ gradient. In the latter case, the permeability coefficient of liposomes to K^+, calculated from the Goldman-Hodgkin-Katz relation, was $6 \cdot 10^{-13}$ m s^{-1}. The selectivity sequence for alkali cations of liposomes was determined from the measured H^+ efflux associated to the influx of the different cations. The selectivity sequence corresponded to the series VI of Eisenman, suggesting interaction of the cation with an anionic field of intermediate strength.

Introduction

Rapid progress in the identification of membrane transport proteins may be expected from recent advances in molecular biology approaches [1,2]. However, development of new biophysical tools, able to give a functional description of the so identified gene-protein structures is lacking behind, especially for the description of electroneutral or poorly electrogenic transport systems reconstituted in proteoliposomes. As facilitated ion fluxes are the difference of overall measured fluxes and non-facilitated ones, the determination of cationic selectivity and permeability coefficients of liposomes are necessary steps before adressing properties of reconstituted transport proteins. Quantitative studies of permeability coefficients and selectivity of liposomes to alkali cations are however scarce and mostly restricted to K^+ and Na^+ [3–10]. The measured permeability coefficients are in the range of 10^{-12} to 10^{-15} m s^{-1}. Neutral liposomes of PC do not discriminate K^+ and Na^+, whereas liposomes of negatively charged PS show a 10-fold higher permeability to K^+ as compared to Na^+ [3]. The analysis of such selectivity requires the study of the complete sequence of alkali cations [11], but this remains a heavy task using radioisotopes. The present paper presents an in vitro analysis of transport of alkali cations using a multichannel photon-counting spectrofluorometer and liposomes multilabelled with fluorescent probes for K^+ (PBFI), H^+ (pyranine) and membrane potential (oxonol VI), designed to permit a detailed quantitative description of ion transport processes on membrane vesicles.

Ion specific fluorescent probes encapsulated into liposomes allow the continuous monitoring at a high sensitivity of the internal content of various ions during filling or emptying experiments. Due to the natural high permeability of liposomes to H^+ [5,7,8,12–14], careful attention has to be paid to the interaction of H^+ and alkali cation fluxes, as well as to the transmembrane electrical effect of pH gradients. Due to the low internal volume of membrane vesicles, transmem-

Correspondence to: R. Gibrat, Biochimie et Physiologie Végétales, ENSA-INRA, Place Viala, F-34060 Montpellier cedex 1, France.

Abbreviations: BTP, 1,3-bis(tris(hydroxymethyl)methylamino)propane; CCCP, carbonylcyanide *m*-chlorophenylhydrazone; DOC, deoxycholate; MLV, multi layer vesicle; PBFI, potassium binding benzofuran isophthalate; SUV, small unilamellar vesicle; TBT, tributyltin chloride; PA, phosphatidic acid; PC, phosphatidylcholine; PS, phosphatidylserine.

brane electrochemical gradients rapidly vanish during filling or emptying experiments. Quantitative analysis of transport processes thus requires that alkali ion and H^+ fluxes, and membrane potential, can be determined simultaneously.

Potassium filling kinetics have been studied in media where K^+ was the only permeant added ion, and thus the K^+ influx was obligatory compensated by an electrically coupled H^+ efflux. Since H^+ efflux mirrors cation influx in this situation, this experimental setup allowed the determination of the relative permeability coefficients of various alkali cations in a rather simple way from the response of the H^+ probe pyranine. The selectivity sequence observed in the present study ($K^+ > Na^+ > Rb^+ > Cs^+ > Li^+$) corresponds to the Eisenman serie VI, reflecting an intermediate anionic field strength.

Materials and Methods

Liposomes. Sonicated liposomes were prepared from 10 mg of egg PC/PG mixtures (8:2, mol/mol) in chloroform. Phospholipids were dried on a vortex mixer under argon to give a thin film on the wall of a glass tube. Phospholipids were subsequently dispersed in 300 μl of the indicated buffers by vigourous mixing on a vortex mixer in the presence of glass beads for 15 min under argon. This suspension of multilayer vesicles (MLV) was sonicated for 15 min under argon in a Bransonic bath sonicator until clarification to obtain small unilamellar vesicles (SUV).

Reconstituted liposomes were obtained from SUV solubilized by deoxycholate (DOC). Solubilization was monitored by measuring the decrease of the turbidity of liposomes in the reconstitution buffer (50 mM histidine-Hepes (pH 6.75), 10% (v/v) glycerol) as a function of detergent concentration (data not shown). Liposomes were fully solubilized at an effective ratio value (R_e = [(detergent) − CMC]/(phospholipid)) of 0.6. Sonicated liposomes (5 mg) were diluted in 1.2 ml reconstitution buffer and an aliquot of DOC (10% w/v) was added to obtain an R_e of 0.6. Disposable syringes (2.5 ml) fitted with porous glass filters were filled with 1.5 ml Sephadex G-50 equilibrated with reconstitution buffer. The syringes were inserted into plastic tubes and centrifuged for 5 min at $180 \times g$ to release extra buffer. Aliquots (220 μl) of the lipid-DOC mixture, prepared as described above, were applied to the columns and centrifuged again. The volumes recovered were within 90% to 100% of the volumes applied.

Encapsulation of PBFI and pyranine in reconstituted liposomes. Liposomes were first reconstituted as described above in the absence of dyes, and concentrated 5-fold by ultrafiltration (Millipore Ultrafree-PF 100,000 NMWL). A PBFI aliquot (1 mM final) and a pyranine aliquot (0.5 mM final) were added to the concentrated liposomes, and the sample was sonicated for 30 s and freeze thawed (liquid nitrogen-room temperature) once. Non encapsulated PBFI and pyranine were removed by chromatography through a Sephadex G-50 column (35 cm × 0.5 cm). As estimated from the fluorescence of the two entrapped dyes, the specific internal volume and radius were, respectively, 4.5 l/mol and 60 nm.

Fluorescence measurements. Fluorescence intensities were measured with a multichannel photoncounting spectrofluorometer SLM-Aminco 8000C interfaced with an IBM computer. The T-shaped configuration of this apparatus allows two simultaneous fluorescence measurements using two channels at emission (channel A and B). Different excitation wavelengths can be rapidly selected during the acquisition cycle with the fast motor driven monochromator (slewing rate 100 nm per s). Acquisition cycles were set-up using the macrocommand programming language available in the SLM software. The data files were further treated (smoothing, calibration, derivation etc.) using SLM software and programs developed in Microsoft Quick Basic. The cuvette was stirred and thermostated at 20°C. The fluorescence signals were ratioed with the signal of the rhodamine reference cell and corrected for the fluorescence of the buffer solutions. In multilabelling experiments, channel B was used alternatively to acquire the PBFI and pyranine signals after excitation at the desired wavelengths. Channel A was used to acquire the oxonol signal.

The maximum of PBFI fluorescence after excitation at 340 nm shifts from 550 nm to 500 nm upon augmentation of the K^+ concentration [15]. We circumvented the shift in emission maximum upon addition of K^+ by using a 495 nm long-pass cut on filter instead of a monochromator at channel B.

Fluorescence intensities of pyranine were measured and stored after excitation at 410 nm, 421 nm and 460 nm, using the same filter and channel.

PBFI was excited at 336 nm, because this wavelength corresponds to one of the two isosbestic excitation wavelengths for pyranine. This allowed the discrimination of PBFI and pyranine signals in multilabelling experiments.

Intensity of the incident light was minimized to prevent photodegradation of the PBFI dye using 2/8 nm input/output slits for the excitation monochromator. During long experiments, illumination of the sample was interrupted between the measurements by shifting the excitation wavelength to 200 nm in combination with a 285 nm long-pass cut on filter at excitation.

The oxonol fluorescence was recorded at 646 nm after excitation at 614 nm, using channel A fitted with a monochromator.

Determination of K^+ and H^+ fluxes, and membrane potential during K^+ influx experiments. Liposomes (80

μg/ml) containing 0.5 mM pyranine and 1 mM PBFI in 50 mM histidine-Hepes (pH 6.75) and 10% (v/v) glycerol were added to the reaction cuvette containing the same buffer and 50 nm oxonol VI. The reaction was started by the addition of 20 mM K_2SO_4 or other SO_4^{2-} salts of alkali cations at the exterior of the vesicles. At the end of the experiment, internal and external media were equilibrated by the addition of DOC (0.05% (w/v)). Internal K^+ and H^+ concentrations, and membrane potential, were determined from calibration plots as described below. The K^+ flux (J_{K^+}) was calculated by derivation of the concentration gradient kinetics determined from the PBFI fluorescence according to the following equation:

$$J_{K^+net} = (V/A)\cdot d([K^+]_{out} - [K^+]_{in})/dt = (r/3)\cdot d\Delta[K^+]/dt \quad (1)$$

where V, A and r are, respectively, the volume, area and radius of the vesicle, and [ ] indicates concentrations.

The net proton flux (J_{H^+net}) was calculated by derivation of the kinetics of pH gradient formation, taking the buffer strength into account according to the following equation [13]:

$$J_{H^+net} = B\cdot(V/A)\cdot dpH/dt = B\cdot(r/3)\cdot dpH/dt \quad (2)$$

The buffer strength (B) was calculated for a two buffer system (C_1 and C_2, respectively, histidine and Hepes):

$$B = 2.3\cdot C_1\cdot D_1\cdot(1-D_1) + 2.3\cdot C_2\cdot D_2\cdot(1-D_2) \quad (3)$$

where D_1 and D_2 are, respectively, $(10^{(pH-pK_1)}+1)^{-1}$ and $(10^{(pH-pK_2)}+1)^{-1}$, and C is the concentration of the buffer. The calculated value for B corresponded accurately with the measured one, using a pK_1 for histidine of 6.0 and a pK_2 for Hepes of 7.5. The contribution of pyranine (0.5 mM) to the buffer strength was negligible.

Other assays. Phospholipid concentration was determined from the phosphorus content of the samples according to the method of Gomori [16].

Results

Calibration of the pH probe pyranine (monolabelling experiments)

Apart from its three sulfonate groups, pyranine possesses one hydroxyl group with a pK of 7.2. The protonated (PyrH) and non-protonated (Pyr^-) forms have different absorbance (i.e., excitation) spectra. The maximum of fluorescence is emitted at 511 nm for both forms, after excitation at 410 nm for PyrH, and at 460 nm for Pyr^-. Pyranine possesses isosbestic points at 336 nm and 421 nm.

Since the fluorescence intensities FI_{460} and FI_{410} are linear [17] with the concentrations of PyrH and Pyr^- (according to the coefficients β and α, respectively), the Henderson-Hasselbach equation can be used to describe the variations of $\log(FI_{460}/FI_{410})$ with pH:

$$\log(FI_{460}/FI_{410}) = pH - pK + \log(\beta/\alpha) = pH - pK' \quad (4)$$

where pK' is the apparent pK, including the constant factor $\log(\beta/\alpha)$ [17].

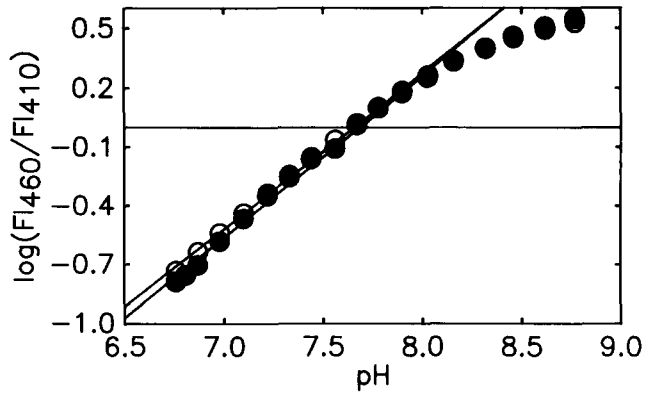

Fig. 1. Effect of pH on the fluorescence of pyranine free in solution or encapsulated into liposomes. Liposomes (80 μg/ml final) containing 50 mM histidine-Hepes (pH 6.75), 10% glycerol (w/v) and 0.5 mM pyranine, were diluted in the same medium without pyranine in the presence of nigericin (0.5 μM). Concentrated aliquots of KOH were added to vary the pH. The catalysed K^+/H^+ exchange allows the free diffusion of KOH to the interior of the vesicles. Pyranine fluorescence was ratioed at 460/410 nm excitation as indicated in Materials and Methods. The logarithm of FI_{460}/FI_{410} was used to calibrate the response of pyranine as a function of pH. The same calibration curves were obtained for pyranine encapsulated into liposomes (•) or free in solution (0.5 μM, ○). No difference was observed for liposomes multilabelled with PBFI and oxonol in addition to pyranine (not shown).

To calibrate the pyranine signal, concentrated KOH aliquots were added to a 50 mM histidine-Hepes buffer (pH 6.75) containing 10% glycerol (w/v) and pyranine in solution (1 μM), or encapsulated in liposomes (0.5 mM). The electroneutral H^+/K^+ exchanger nigericin was added to liposomes, to allow a free equilibration of KOH. The results in Fig. 1 confirm that relation (4) can be used to fit the pH dependence of the pyranine fluorescence around the pK [13,17]. No difference was observed between pyranine free in solution or encapsulated into liposomes.

The value of $\log(FI_{460}/FI_{410})$ was strongly dependent on the K^+ concentration (Fig. 2). This was due to an aspecific ionic strength effect, since the same effect was observed with other monovalent cations (data not shown). This ionic strength effect was further studied in relation with the pH dependence of $\log(FI_{460}/FI_{410})$, using different proportions of histidine and Hepes buffers (50 mM total in 10% glycerol) and varying, for each proportion, the ionic strength (KCl). This resulted in a series of parallel calibration curves of $\log(FI_{460}/FI_{410})$ versus pH for different ionic strengths (not shown). The apparent pK value of pyranine (pK'),

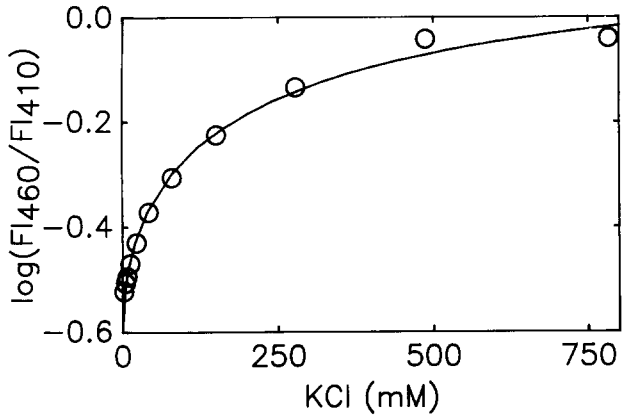

Fig. 2. Effect of the ionic strength on the pyranine fluorescence. The fluorescence ratio FI_{460}/FI_{410} of free pyranine (0.5 μM) in 50 mM histidine-Hepes (pH 6.75) and 10% (v/v) glycerol was measured as indicated in Materials and Methods. The ionic strength was varied by the addition of KCl. Other alkali cations had the same effect (not shown). Solid line: calculated curve by fitting the experimental data by non-linear regression analysis using Eqn. 10 obtained from the Debye-Huckel treatment of the ionic strength, with $pK_i' = 7.11$, $A = 0.866$ and $A' = 0.065$.

calculated using Eqn. 4, diminished when the K^+ concentration increased (Fig. 3).

This ionic strength effect was analyzed according to the Debye-Huckel theory [18]. Protons will be accumulated in the vicinity of the strongly negatively ionized pyranine (valency $z_p = -4$ or -3 depending on pH), according to the following Boltzman distribution law, where ϕ is the (negative) electrostatic potential considered at the distance r from the reference ion pyranine,

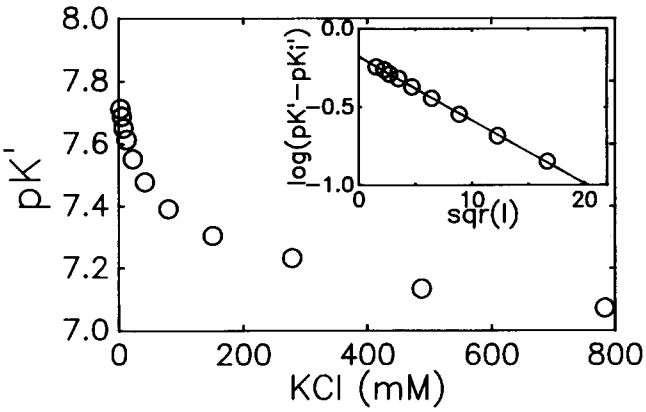

Fig. 3. Effect of the ionic strength on the apparent dissociation constant for H^+ (pK') of pyranine. Fluorescence of free pyranine (0.5 μM) was measured as indicated in the text, in 50 mM histidine-Hepes and 10% (v/v) glycerol. The pH was varied by varying the ratio histidine/Hepes, whilst ionic strength was varied by addition of KCl. The value of pK' was determined from a plot of $\log(FI_{460}/FI_{410})$ vs. pH according to Eqn. 4 for different ionic strength. With augmenting ionic strength (I), the apparent value (pK') diminishes towards the intrinsic value ($pK_i' = 7.07$) (Eqn. 9). The plot of $\log(pK' - pKi')$ vs. $\sqrt{I}$ was linear (inset) and allowed to calculate the parameters A (0.747) and A' (0.0934) from, respectively, the intercept with the y-axis and the slope of the regression line.

k, and T are the classical thermodynamic constants, and e_o is the unit electrostatic charge:

$$[H^+]_r = [H^+]_b \cdot \exp(-e_o \cdot \phi / kT) \quad (5)$$

Thus, the local proton concentration actually perceived by the pyranine dye depends on both the proton concentration in the bulk (H_b^+) and the value of the electrostatic potential ϕ. The latter can be estimated using the linearized Poisson-Boltzman equation, where z_p is the valency of the reference ion pyranine, ϵ the dielectric constant of the medium, I the ionic strength and K^{-1} is the Debye-Huckel reciprocal length:

$$\phi = (z_p e_o / \epsilon r) \exp(-Kr) \quad (6)$$

with:

$$K = \sqrt{((4\pi/\epsilon kT) \cdot 2 \cdot I \cdot e_o^2)} \quad (7)$$

combining Eqns. 4 to 7 gives:

$$\log(FI_{460}/FI_{410}) = pH_b - pK_i + \log(\beta/\alpha) - A \cdot \exp(-A'\sqrt{I}) \quad (8)$$

with:

$$A = 0.43(z_r^2 e_o^2 / \epsilon r k T) \text{ and } A' = r\sqrt{(8\pi e_o^2 / \epsilon k T)}$$

where pK_i is the 'intrinsic' dissociation constant of pyranine (i.e., the one in the absence of electrostatic interactions). Finally, the apparent pK' of the pyranine dye experimentally determined from the value of $\log(FI_{460}/FI_{410})$ versus pH should depend on its intrinsic value, on the parameters β and α, and on the ionic strength according to:

$$pK' = pK_i - \log(\beta/\alpha) + A \cdot \exp(-A'\sqrt{I}) = pK_i' + A \cdot \exp(-A'\sqrt{I}) \quad (9)$$

A decrease of pK' with augmenting ionic strength is predicted by Eqn. 9, as experimentally observed (Fig. 3). At higher ionic strength, pK' should approach the value of pK_i'. From this experimentally estimated pK_i' value, the observed difference $\log(pK' - pK_i')$ should be linear with $\sqrt{I}$, which was actually observed (Fig. 3, inset). The value of the constants A and A', determined respectively from the slope and the intercept of the regression line could be used to fit accurately the experimental data (see theoretical curve in Fig. 2).

Calibration of the K^+ probe PBFI (monolabelling experiments)

The PBFI molecule is a crown ether compound, linked via its nitrogens to benzofuran fluorophores bearing isophthalate groups as additional liganding

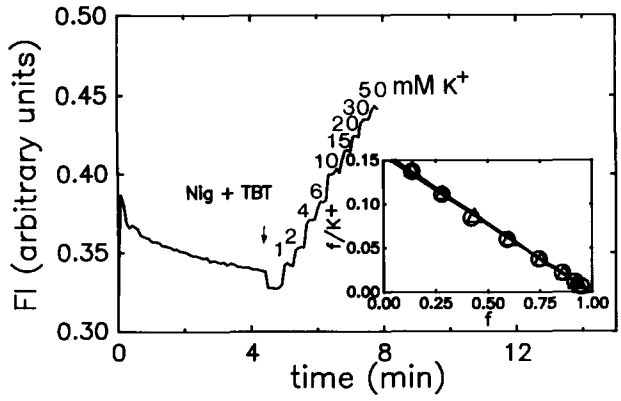

Fig. 4. Calibration of the fluorescence of PBFI encapsulated in liposomes and free in solution as a function of K^+ concentration. Liposomes (80 μg/ml final) containing 50 mM histidine-Hepes (pH 6.75), 10% glycerol (w/v) and 1 mM PBFI were diluted in the same medium without PBFI. Nigericin (0.5 μM; H^+/K^+ exchange) and TBT (0.5 mM; Cl^-/OH^- exchange) were added to equilibrate internal and external K^+ concentrations. The initial diminution of the PBFI signal was caused by an internal K^+ contamination (associated to the lipids). Thereafter aliquots of concentrated KCl were added to the medium to calibrate the PBFI signal as a function of the internal K^+ concentration. Inset: Scatchard plot of PBFI fluorescence with K^+ concentration for encapsulated ($\triangle$) or 2 μM free probe probe (○). The parameter f is defined as $(FI_{K^+} - FI_o)/(FI_{max} - FI_o)$, where FI_o and FI_{max} are, respectively, the PBFI fluorescence in the absence of K^+ or in the presence of a saturating K^+ concentration. Similar results were obtained when liposomes were multilabeled with pyranine and oxonol (not shown).

centers [19]. It binds K^+ according to a mass action law:

$$K_{d,app} = ([PBFI] \cdot [K^+])/[KPBFI] \quad (10)$$

The fluorescence of the KPBFI complex is higher than that of free PBFI. Fluorescence increases with the concentration of KPBFI, according to the following equation, where FI_o and FI_K are respectively the fluorescence of the dye in the absence and in the presence of K^+, and γ is a constant [15]:

$$FI_K = FI_o + \gamma \cdot [KPBFI] \quad (11)$$

The binding isotherm in terms of fluorescence is:

$$(FI_K - FI_o) = (FI_{max} - FI_o) \cdot [K^+]/(K_{d,app} + [K^+]) \quad (12)$$

Potassium titration of PBFI fluorescence with concentrated KCl aliquots allowed to determine FI_o, FI_{max} and K_d using a Scatchard plot (Fig. 4). When encapsulated in liposomes, PBFI was titrated in the presence of 0.5 μM nigericin and 0.5 mM TBT as described by Jezek et al. [15]. The combination of K^+/H^+ and Cl^-/OH^- antiporters permits the free equilibration of KCl across the lipidic membrane. The same K_d values were determined for free or encapsulated PBFI in 50 mM histidine-Hepes (pH 6.75) and 10% (v/v) glycerol (Fig. 4, inset).

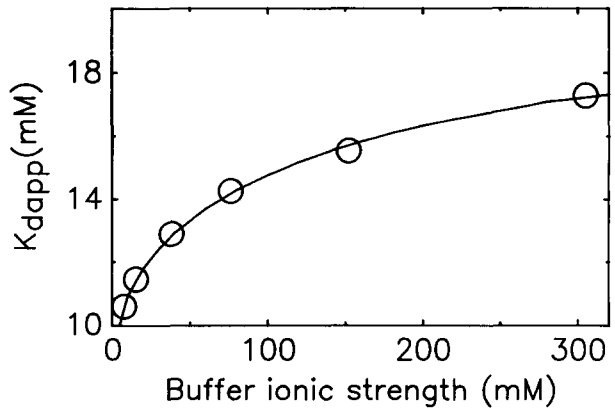

Fig. 5. Effect of the buffer ionic strength on the apparent dissociation constant ($K_{d,app}$) of free PBFI for K^+. Free PBFI (2 μM) in various BTP-SO_4 (pH 6.75) concentrations was titrated with KCl and the value of $K_{d,app}$ was determined from Eqn. 12. The data were fitted by non-linear regression to the theoretical relation for the ionic strength effect of the buffer according to the Debye-Huckel theory (solid line: $K_{d,app} = A \cdot K_d \cdot \exp(-A' \cdot \exp(A'' \cdot \sqrt{I}))$ with $A \cdot K_d$ = 19.56 mM, $A' = 0.81$, and $A'' = -0.11$).

The dependence of $K_{d,app}$ of PBFI on the ionic strength of the medium has been examined by titrating the free probe with KCl in BTP-Cl (pH 6.75), for a buffer ionic strength in the range of 5 to 300 mM. As for pyranine, the value of $K_{d,app}$ increased upon augmentation of the buffer ionic strength, accordingly to the Debye-Huckel theory (Fig. 5).

Using histidine-Hepes buffers at different pH values but at a constant ionic strength, it was observed that the value of $K_{d,app}$ rapidly increased when the medium was acidified (Fig. 6), whilst the value of FI_o and FI_{max} remained almost unaffected (not shown). At a given

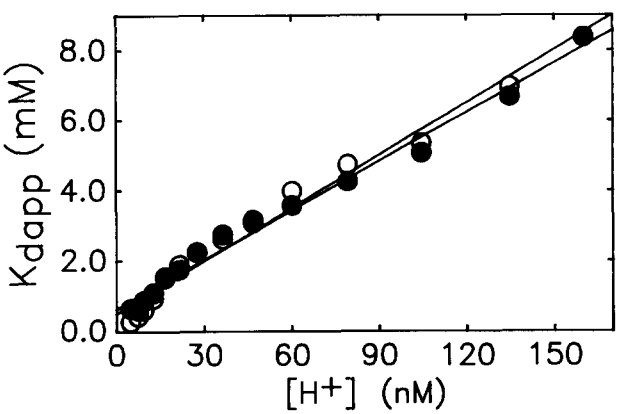

Fig. 6. pH dependence of the apparent dissociation constant for K^+ of PBFI encapsulated or free in solution. Encapsulated PBFI (●) was calibrated using liposomes (80 μg/ml) containing 1 mM PBFI and 0.5 mM pyranine in 50 mM histidine-Hepes (pH 6.75), 10% (v/v) glycerol and nigericin (0.5 μM). This K^+/H^+ exchanger allowed to equilibrate various K^+ concentrations by adding KOH aliquots at the exterior. The value of $K_{d,app}$ was calculated as indicated in the text from the Eqn. 14. The internal pH was simultaneously determined from the fluorescence of the pyranine dye. Free PBFI (○) was calibrated in the same buffer by adding KOH aliquots. From Eqn. 15 values of $0.7 \cdot 10^{-3}$ and $1.5 \cdot 10^{-8}$ M were obtained for $K_{d,K}$ and $K_{d,H}$ respectively.

ionic strength, this increase of $K_{d,app}$ could be described assuming a competition of H^+ and K^+ for the binding site. Noting $K_{d,K}$ the dissociation constant for K^+ and $K_{d,H}$ the dissociation constant for H^+, the binding equation is given by:

$$[K^+] = (K_{d,K} + K_{d,K} \cdot [H^+]/K_{d,H})/((FI_{max} - FI_K)/(FI_K - FI_o)) \quad (13)$$

$$[K^+] = K_{d,app}/((FI_{max} - FI_K)/(FI_K - FI_o)) \quad (14)$$

with:

$$K_{d,app} = K_{d,K} + K_{d,K} \cdot [H^+]/K_{d,H} \quad (15)$$

The plot of $K_{d,app}$ vs. H^+ actually gave a straight line from which $K_{d,K}$ and $K_{d,H}$ can be calculated (Fig. 6). For both free and encapsulated PBFI, similar $K_{d,K}$ and $K_{d,H}$ values were obtained.

In conclusion, careful attention has to be paid to ionic strength effects of monovalent salts on the response of both dyes pyranine and PBFI. The theoretical frame of Debye-Huckel gives a powerful rationale to describe and predict such aspecific effects. This is useful when transport experiments involve variations of ionic strength at the interior of the vesicles. In the following experiments, ionic strength was maintained at a constant value: since K^+ was the only permeant species added to the external medium, the entry of K^+ into the vesicles was compensated by an equivalent H^+ efflux. Formally, the increase in K^+ concentration in the vesicles was electrically compensated by an equivalent decrease of the cationic forms of the buffer.

Calibration of the oxonol VI probe (monolabelling experiments)

The fluorescence of the lipophilic anion oxonol VI was measured at excitation/emission wavelengths of 614/646 nm, corresponding to the maximum relative variation of the fluorescence upon its binding to liposomes (not shown). The response of oxonol to an inside positive membrane potential results from an augmentation of its binding to the internal leaflet of the membrane vesicle [20]. Fluorescence was expressed as the ratio of fluorescence augmentation (ΔFI) to basal fluorescence at zero membrane potential (FI_o). The standard assay medium (2 ml) contained 50 mM histidine-Hepes (pH 6.75), 10% (v/v) glycerol and 50 nM oxonol. This low oxonol concentration was used to prevent dissipation of the inside positive membrane potential by the anionic conductance of the probe. The probe was calibrated using imposed K^+ gradients (SO_4^{2-} salt) in the presence of valinomycin (Fig. 7). A linear relation was observed between $\Delta FI/FI_o$ and the theoretical membrane potential (Fig. 7, inset) as expected from the mechanism of the response of the dye [20].

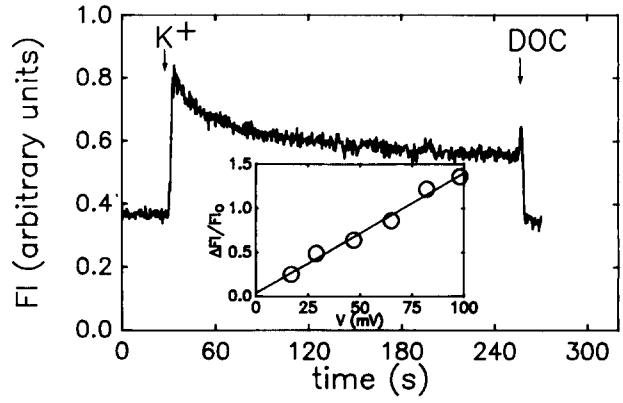

Fig. 7. Calibration of the oxonol VI fluorescence as a function of imposed K^+ diffusion gradient in the presence of valinomycin. Liposomes (80 μg/ml prepared in 50 mM histidine-Hepes (pH 6.75), 10% (v/v) glycerol and 0.5 mM K_2SO_4 were diluted in the same medium plus 0.1 μM valinomycin and 50 nM oxonol VI. The K^+ diffusion membrane potential was created by addition of a concentrated aliquot of K_2SO_4 in the external medium. Thereafter, the membrane potential was collapsed by addition of 0.01% DOC (w/v). Inset: the maximum fluorescence minus the fluorescence in the presence of DOC (ΔFI) divided by the fluorescence in the presence of DOC (FI_0) was used to calibrate the oxonol response as a function of the K^+ diffusion potential (V) calculated from the Nernst equation.

Spectral analysis and calibration procedures for multilabelled liposomes

Fig. 8 shows the corrected excitation spectra of pyranine (0.5 μM) or PBFI (1 μM) in 50 mM histidine-Hepes (at various pH values) and 10% (v/v) glycerol, or both probes together. These spectra are corrected for blanks and ratioed with the fluorescence of the rhodamine reference cell. The sum of the spectra obtained with the probes individually was identical to the spectrum obtained with a mixture of probes. Addition of oxonol, did not modify the spectra of pyranine and PBFI (not shown). PBFI, pyranine and oxonol fluorescences were measured as indicated in Materials and Methods. A 336 nm wavelength was retained for the excitation of PBFI, since it corresponds to the isosbest of pyranine being closest to the maximum excitation wavelength of PBFI (340 nm). At 336 nm, the small contribution of pyranine to the PBFI signal was independent of the internal pH.

To circumvent the effects of varying ionic strength on PBFI and pyranine, the following dual calibration procedure was used for multilabelled liposomes. Concentrated KOH aliquots were added in the presence of the electroneutral H^+/K^+ exchanger nigericin. Since the equilibration of the vesicles resulted from a H^+/K^+ exchange, the ionic strength inside the vesicles remained unchanged. Furthermore, due to the buffer strength used, the quasi-totality of K^+, initially added with OH^-, was neutralized by the anionic form of the Hepes buffer, following its deprotonation upon OH^- addition: the bulk ionic strength itself was not signifi-

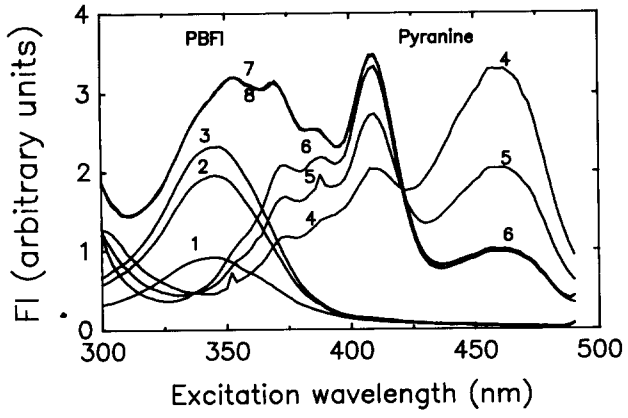

Fig. 8. Comparison of the excitation spectra of free pyranine and PBFI, and of the mixture of the two probes. The excitation spectra of 1 μM PBFI, with 2, 20 and 40 mM K^+ (traces 1 to 3) and 0.5 μM pyranine at pH 6.75, 7.50 and 8.00, (traces 4 to 6) were measured in 50 mM histidine-Hepes and 10% (v/v) glycerol using channel B and a 495 nm long-pass cut on filter (see Materials and Methods). The spectra were corrected for the fluorescence of the buffer solutions and ratioed with the fluorescence of the rhodamine reference cell. No difference was observed between the mathematical sum of the spectra of free pyranine and PBFI measured individually (trace 7 = sum of traces 3 and 6), and the spectrum of a mixture of PBFI and pyranine (trace 8). Routinely the isosbestic point of pyranine at 336 nm was used to excite the PBFI probe to determine K^+ concentration without interference of the response of pyranine fluorescence to pH. The isosbestic point at 421 nm was used to ratio the PBFI fluorescence. pH dependent pyranine fluorescence was measured at 410 and 460 nm as indicated in the text.

cantly modified. Anew, no difference was observed when calibration of the probes was performed with free or encapsulated dyes (not shown). The proton concentration was calculated from the pyranine fluorescence for a constant ionic strength using the determined value of pK' from Eqn. 4.

FI_o, FI_{max} and $K_{d,app}$ for PBFI fluorescence were determined directly from the calibration plot from Eqn. 12 and the parameters $K_{d,H}$ and $K_{d,K}$ were calculated from Eqn. 15. After calibration of the probes, the internal K^+ concentration was determined from Eqn. 13. The value of I was considered constant during the influx experiment and equal to the initial internal ionic strength.

Simultaneous measurements of K^+ influx, H^+ efflux and membrane potential

Internal K^+ and H^+ concentrations, and membrane potential, were determined according to the above described procedures, after addition of 20 mM K_2SO_4 at the exterior of the vesicles, both in the presence and absence of valinomycin. In the presence of valinomycin, a high membrane potential was determined from the response of the oxonol probe (Fig. 9A). The diffusion potential decayed slowly while a pH gradient was built. After approx. 100 min both H^+ and K^+ were at a quasi thermodynamical equilibrium. During the whole kinetics, the value given by the oxonol probe was close to the theoretical Nernst potential calculated from the observed K^+ gradient (determined from the PBFI fluorescence).

In the absence of valinomycin, the initial value of the membrane potential was null in the presence of the protonophore CCCP (not shown), and about 10 mV in its absence (Fig. 9B). However, a time-dependent increase of the membrane potential was observed, in contrast to the decrease previously observed in the presence of valinomycin. The maximum size of the membrane potential was in accordance with the calculated Nernst potential for the built H^+ gradient, measured with the pyranine probe. It reached the same stationnary level as the one previously observed in the presence of valinomycin.

The K^+ and H^+ net fluxes were calculated as indicated in Materials and Methods. The initial K^+ and H^+ fluxes were electrically coupled, in the absence of valinomycin, by a small membrane potential (Fig. 9). This permits to use the value of the initial flux (J_{ini})

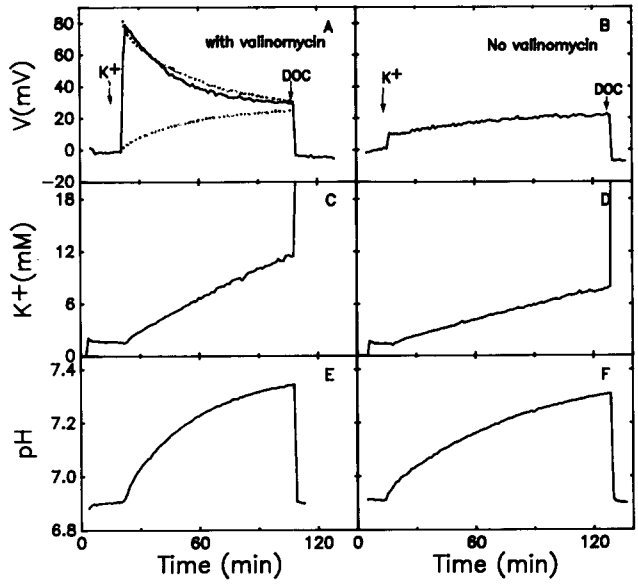

Fig. 9. Simultaneous determinations of membrane potential, internal pH and K^+ concentration during K^+ filling kinetics of liposomes, using the probes oxonol VI, pyranine and PBFI. Liposomes (80 μg/ml) containing 50 mM histidine-Hepes (pH 6.75), 10% (v/v) glycerol, 1 mM PBFI and 0.5 mM pyranine, were diluted into 50 mM histidine-Hepes (pH 6.75), 10% (v/v) glycerol and 50 nM oxonol VI. Calibration of the probe signals and fluorescence measurements were performed as described in the precedent figures and in Materials and Methods. The reaction was started by addition of 20 mM K_2SO_4 in the medium in the presence (left panels) or absence (right panels) of valinomycin. At the end of the experiment, internal and external ionic conditions were equilibrated by addition of DOC (0.05% w/v). Panels A and B: membrane potential measured with the oxonol probe (solid line), or calculated from the K^+ diffusion gradient (A, upper dotted line) or from the H^+ diffusion gradient (A, lower dotted line). Panels C and D: internal K^+ concentration measured with the PBFI probe. Panels E and F: internal pH measured with the pyranine probe.

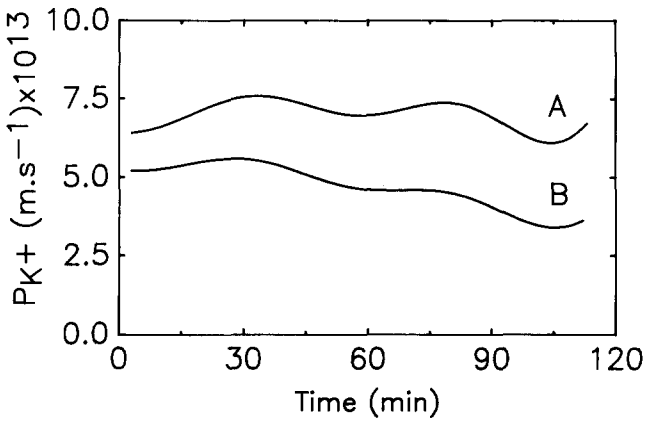

Fig. 10. K^+ permeability coefficient determined from simultaneous measurements of K^+ flux and membrane potential. Liposomes (80 μg/ml) containing 50 mM histidine-Hepes (pH 6.75), 10% (v/v) glycerol, 1 mM PBFI and 0.5 mM pyranine were diluted into 50 mM histidine-Hepes (pH 6.75) and 10% (v/v) glycerol and 0.2 μM CCCP. K^+ fluxes and membrane potential were calculated as indicated in Materials and Methods. The K^+ permeability coefficient was determined according to Fick's law (Eqn. 16 trace B), or by correcting for the measured membrane potential according to the Goldman-Hodgkin-Katz equation (Eqn. 17 trace A).

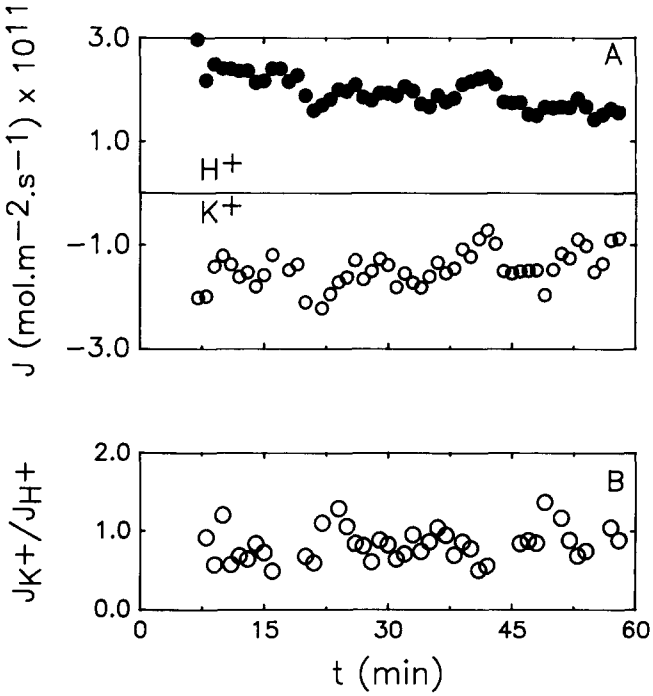

Fig. 11. K^+ and H^+ fluxes respectively measured with the PBFI and pyranine probes during a K^+ filling experiment. Liposomes (80 μg/ml) containing 50 mM histidine-Hepes (pH 6.75), 10% (v/v) glycerol, 1 mM PBFI and 0.5 mM pyranine were diluted into 50 mM histidine-Hepes (pH 6.75) and 10% (v/v) glycerol. The reaction was started by addition of 20 mM K_2SO_4 at the exterior. K^+ and H^+ fluxes were calculated from the derivation of the measured internal K^+ and H^+ concentrations as explained in Materials and Methods (Eqns. 1 and 2). (A) Upper panel: H^+ flux. Lower panel: K^+ flux. (B) Ratio of H^+ flux and K^+ flux.

together with the Fick's law (used for electroneutral diffusion), to approximate the permeability coefficient to K^+ (P_K) of the membrane:

$$P_K = J_{ini}/\Delta[K^+] \tag{16}$$

In the presence of a membrane potential, the permeability coefficient can be corrected, using the Goldman-Hodgkin-Katz equation:

$$P_K = J_K(RT/VF)(\exp(VF/RT)-1)$$
$$\times[([K^+]_{in}\cdot\exp(VF/RT)-[K^+]_{out})]^{-1} \tag{17}$$

in which R, T and F are the classical thermodynamical parameters, J_K is the K^+ flux, V is the membrane potential and $[K^+]_{in}$ and $[K^+]_{out}$ represent, respectively, the internal and external K^+ concentrations.

However, this procedure is useful only when the membrane potential is not too close to the one determined by the K^+ diffusion gradient. In the latter case (for instance in the presence of valinomycin) the value of the denominator in Eqn. 17 will be close to zero, resulting in large variations in the calculated P_K, upon small variations in the experimentally determined K^+ concentrations and membrane potential.

Fig. 10 shows that such a correction allows to calculate the permeability coefficient over a prolonged time period during a K^+ influx experiment in the absence of valinomycin. A permeability coefficient to K^+ of $(6 \pm 3)\cdot 10^{-13}$ m s^{-1} at 20°C was obtained from this relation.

Furthermore, net K^+ and H^+ fluxes exhibited a stoichiometry close to 1:1 (Fig. 11). This was expected

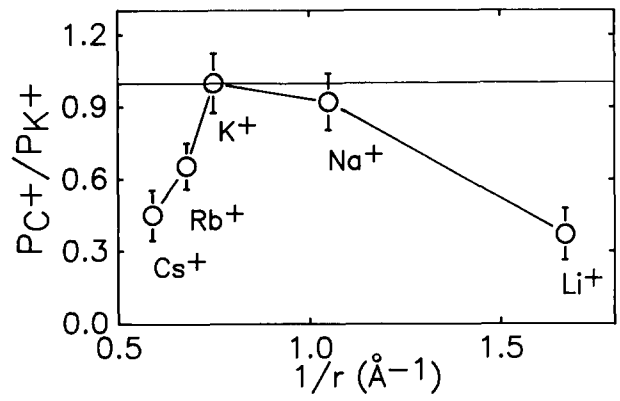

Fig. 12. Permeability coefficients of liposomes to alkali cations. Liposomes (80 μg/ml) containing 50 mM histidine-Hepes (pH 6.75), 10% (v/v) glycerol and 0.5 mM pyranine were diluted in 50 mM histidine-Hepes (pH 6.75) and 10% (v/v) glycerol at 45°C. The reaction was started by addition of 40 mM of alkali cations (as SO_4^{2-} salts) in the medium. The measured proton efflux mirrored the equivalent net cation influx, as shown in Fig. 11, and allowed to estimate the permeability coefficients as indicated in the text. The permeability coefficients were plotted as a function of the reciprocal ionic radius of the different alkali cations. The data represent the mean of three independent repetitions.

since K^+ and H^+ were the only significant permeant ions in the medium. Since the K^+ and H^+ fluxes are mirror images, the latter can also be used to estimate the permeability of the membrane to K^+ and to other cations. In this way we used the pH dye pyranine to study the cationic selectivity of the membrane, measuring the net H^+ fluxes developed after imposition of a cation gradient (Fig. 12). From all tested ions, K^+ was the most permeant one, whilst the ionic selectivity sequence was: $K^+ > Na^+ > Rb^+ > Cs^+ > Li^+$, which corresponds to the Eisenman series VI [11].

Discussion

Validity of the spectroscopic methods

Impermeant fluorescent dyes are generally highly ionized molecules. The observed ionic strength effects on the response of pyranine and PBFI dyes indicate that electrostatic interactions are to be taken into account for quantitative analysis. Of course, maintaining the ionic strength at a constant value would be the best way to overcome this difficulty. But, if impossible, the Debye-Huckel theory provides a convenient conceptual frame to describe, and correct for ionic strength effects.

The design of impermeant ion specific dyes generally involves ionized binding sites. Thus, competition of H^+ and the specific ion of interest, as observed for PBFI, can be considered as another general behaviour to be taken into account for quantitative analysis. To face this difficulty, the simultaneous use of the ion specific probe and a pH probe permits to correct for the competiting effect of H^+.

Calibration of the probes, encapsulated or free in solution did not give significant differences in monolabelled or in multilabelled samples (Figs. 1, 6, 8). The internal K^+ concentration in filling kinetics, determined from the PBFI fluorescence, reached a final equilibrium value which is in good agreement with the known concentration of K^+ initially added outside (Fig. 9). Furthermore, the K^+ and H^+ fluxes as estimated from the PBFI and the pyranine fluorescences respectively could reasonably be considered to be mirror images, as was to be expected to garanty electroneutrality in the absence of other permeant ionic species (Fig. 11).

The oxonol VI probe is also usable for the quantitative determination of the membrane potential, provided that its conductance is reduced using very low concentrations of oxonol (10 nM range). In these conditions, the theoretical potential calculated in K^+ filling kinetics from the measured K^+ gradient (PBFI dye) in the presence of valinomycin is close to the potential given by the probe (Fig. 9), whilst in the absence of valinomycin the potential is close to the one calculated from the pH gradient (pyranine).

The validity of the different quantitative methods, which include encapsulation, acquisition and correction procedures, as well as mathematical treatment of signals (calibration, derivatives etc.) is thus a posteriori attested by the overall physical consistency of the various parameters.

In conclusion, apart from methodological advantages (for example, correction for H^+ competiting effects), the use of multilabelled vesicles allows to gain simultaneously and quantitatively three pieces of information: the ionic transport of interest, the coupled cotransport and their transmembrane electrical effects.

Transmembrane electrical effects

In the absence of valinomycin, the membrane potential determined with the oxonol probe after the imposition of an inward K^+ diffusion gradient was about 10 mV (Fig. 9B). Indeed, the permeability coefficient to H^+ of liposomes has been shown to be about one million times as high as compared to other univalent ions, including K^+ [5,7,8,12–14]. Thus, the membrane conductance to protons was much higher than that to K^+, in spite of the very low H^+, and high K^+, concentrations in the medium, and efficiently short-circuited the membrane potential.

An important consequence of the natural high H^+ conductance of liposomes is that the membrane potential was negligible only at the begining of K^+ filling experiments. The size of the membrane potential increased in agreement with the theoretical (Nernst) membrane potential for the observed pH gradient built by the K^+/H^+ exchange in these experiments (Fig. 9A, B). A stationary state was reached where the membrane potential corresponded to the quasi-equilibrium potential for both H^+ and K^+ ions.

The H^+ conductance became truly negligible as compared to the K^+ conductance when valinomycin was present: the value of the membrane potential following the imposition of a K^+ gradient was almost instantaneously established, and was in good agreement with the Nernst potential calculated from the measured K^+ gradient (Fig. 9A).

Quantitative analysis of permeability coefficient and cationic selectivity of liposomes

Data in literature on ionic permeability coefficients, and ionic selectivity in liposomes are scarce and variable. The permeability coefficient of phosphatidylcholine lipid bilayers for Na^+ and K^+ are variable (10^{-14} m s^{-1} [4]; 10^{-12} m s^{-1} [8]; $0.3 \cdot 10^{-12}$ to $2.7 \cdot 10^{-12}$ m s^{-1} [5]). This variability is probably caused by the difference in used lipids, as well as in the methods to estimate the permeability coefficient. Another source of variation is the type of liposomes used. Elimination of detergent and prevention of oxidation of lipids during preparation is crucial for a high permeability bar-

rier [12,22]. In the present study, we determined the ionic permeability coefficient of liposomes of PC/PG (8:2, mol/mol), from the measured K^+ and H^+ fluxes, taking the membrane potential into account. As shown above, the oxonol probe gave reliable determinations of the membrane potential during K^+ filling experiments, and allowed to calculate the permeability coefficient from the measured K^+ flux according to the Goldman-Hodgkin-Katz equation.

The net K^+ flux could be measured directly using PBFI, but also indirectly from the net H^+ flux measured with the pH probe pyranine (Fig. 11). The validity of this procedure is shown by the near 1:1 stoichiometry of the net K^+ and H^+ fluxes. This procedure allowed the determination of the permeability coefficients to other alkali cations for which no ion specific probes are available. (Only the Na^+ specific probe SBFI, which is similar to PBFI, is at present available, and could thus be used to further verify the assertion that Na^+ and H^+ flux mirror one another.) The permeability coefficient to Na^+ ($5 \cdot 10^{-13}$ m s^{-1}), was in the range of the values (approx. $0.3 \cdot 10^{-12}$ to $3 \cdot 10^{-12}$ m s^{-1}) obtained from self-diffusion experiments of ^{22}Na across PC/PA (98:2, mol/mol) large unilamellar liposomes [8], or across Black Lipidic Membrane of PC [5]. The liposomes used in the present study (PC/PG 8:2, mol/mol) exhibited a cationic selectivity in favor of K^+ ($K^+/Na^+/Rb^+/Cs^+/Li^+ = 1:0.92:0.66:0.45:0.37$; Fig. 12).

In order to explain this selectivity, ionic radius of hydrated and non hydrated ions as well as anionic electrical field strength at the membrane interface has to be considered. Partial hydratation of ions can minimize the transfer energy for an ion in the lipid bilayer, diminishing electrostatic energy but augmenting surface energy [21]. All ions will therefore tend to be at their lowest energy state in a sphere of water of the same size. This would explain the absence of selectivity of neutral bilayers as observed in literature [3].

Nevertheless, a 10-fold discrimination of K^+ over Na^+ has been observed for liposomes of the negatively charged PS [3]. Such discrimination can be interpreted considering the anionic field strength of the polar head of the phospholipids [11], provided that the complete sequence of alkali cations could be examined. The moderatly charged liposomes (PC/PG (8:2, mol/mol)) used in the present study also discriminate K^+ over Na^+ according to the Eisenman serie VI, reflecting an intermediate anionic field strength at the membrane surface. The magnitude of the K^+/Na^+ discrimination observed in this study is much lower than the one reported above for liposomes of PS. It has to be pointed out that the magnitude of such discrimination should strongy depend on the hydration of the interacting anion.

In conclusion, membrane vesicles multilabelled with ion specific and membrane potential probes, monitored with a multichannel spectrofluorometer, offer the possibility to measure K^+ and H^+ fluxes and the membrane potential, continuously and simultaneously. The consistency of the different parameters with the Goldman-Hodgkin-Katz relation indicates that an electrophysiological analysis can be developed to study ion transport processes on isolated membrane vesicles. Facilitated ionic fluxes supported by reconstituted transport proteins are determined as the difference of overall measured fluxes and non-facilitated ones. The present study on liposomes is therefore the first step before adressing transport properties of reconstituted proteins.

References

1 Sentenac, H., Bonnaud, N., Minet, M., Lacroute, F., Salmon, J.-M., Gaymard, F. and Grignon, C. (1992) Science 256, 663–664.
2 Anderson, J.A., Huprikar, S.S., Kochian, L.V., Lucas, W.J. and Gaber, R.F. (1992) Proc. Natl. Acad. Sci. USA 89, 3736–3740.
3 Papahadjopoulos, D. (1971) Biochim. Biophys. Acta 241, 254–259.
4 Deamer, D.W. and Bramhall, J. (1986) Chem. Phys. Lipids 40, 167–188.
5 Gutknecht, J. and Walter, A. (1981) Biochim. Biophys. Acta 641, 183–188.
6 Gutknecht, J. (1984) J. Membr. Biol. 82, 105–112.
7 Gutknecht, J. (1987) Biochim. Biophys. Acta 898, 97–108.
8 Nichols, J.W., Hill, L.W., Bangham, A.D. and Deamer, D.W. (1980) Biochim. Biophys. Acta 596, 393–403.
9 Nichols, J.W. and Deamer, D.W. (1980) Proc. Natl. Acad. Sci. USA 78, 4324–4328.
10 Deamer, D.W. (1987) J. Bioenerg. Biomembr. 19, 457–479.
11 Eisenman, G. (1960) in Membrane Transport and Metabolism (Kleinzeller, A. and Kotyk, A., eds.), pp. 163–179, Academic Press, New York.
12 Perkins, W.R. and Cafiso, D.S. (1986) Biochemistry 25, 2270–2276.
13 Rossignol, M., Thomas, P. and Grignon, C. (1982) Biochim. Biophys. Acta 684, 195–199.
14 Norris, F.A. and Powell, G.L. (1990) Biochim. Biophys. Acta 1030, 165–171.
15 Jezek, P., Mahdi, F. and Garlid, K.D. (1990) J. Biol. Chem. 265, 10522–10526.
16 Gomori, G. (1942) J. Lab. Clin. Med. 27, 955–960.
17 Kano, K. and Fendler, J.H. (1978) Biochim. Biophys. Acta 509, 289–299.
18 Bockris, J. O'M. and Reddy, A.K.N. (1970) in Modern Electrochemistry, (Bockris, J.O'M. and Reddy, A.K.N., eds.), Vol. 1, Plenum Press, New York.
19 Minta, A. and Tsien, R.Y. (1989) J. Biol. Chem. 264, 19449–19457.
20 Apell, H.J. and Bersch, B. (1987) Biochim. Biophys. Acta 903, 480–494.
21 Macdonald, R., (1976) Biochim. Biophys. Acta 448, 193–198
22 Rigaud, J.L., Levy, D. and Seigneuret, M. (1991) Trends Biomembr. Bioenerg. 1, 11–27.